Available online at www.sciencedirect.com
ScienceDirect
Ceramics International 37 (2011) 3523–3529
CERAMICS INTERNATIONAL
www.elsevier.com/locate/ceramint

Synthesis of mono-dispersed spherical Nd:Y_2O_3 powder for transparent ceramics

Yihua Huang *, Dongliang Jiang, Jingxian Zhang, Qingling Lin, Zhengren Huang

The State Key Laboratory of High Performance Ceramics and Superfine Structure, Shanghai Institute of Ceramics, Shanghai 200050, China

Received 10 May 2011; received in revised form 3 June 2011; accepted 3 June 2011
Available online 12 June 2011

Abstract

Transparent Nd:Y_2O_3 ceramic was obtained by sintering mono-sized spherical powder. The powder was prepared by homogeneous precipitation method in aqueous media using urea to regulate the pH. The structure and morphology of the powder were investigated by TG–DTA, XRD, SEM and IR spectrum. The effect of aging temperature, time, and the concentration of urea, [Y^{3+}], and [Nd^{3+}] were investigated. Results showed that the obtained precursor was $R_2(OH)CO_3{\cdot}H_2O$ (R = Y, Nd), and the least size of mono-sized spherical yttria particles was 72 nm by a microwave oven method after calcinations at 850 °C for 4 h. After dry press and CIP, the particles accumulated closely, and no defects can be detected in the green body.

Keywords: Nd:Y_2O_3; Transparent ceramics; Mono-sized powder

1. Introduction

Transparent poly-crystalline yttria (of cubic lattice structure) [1–3] has been investigated for a long time as an active host material for lanthanide ions due to its excellent properties such as heat resistance, stability and optical clarity over a broad spectral region. Because of its high thermal conductivity, yttria is a promising host material for solid-state laser [4], which makes it capable to endure more energy from laser radiation. And its thermal expansion coefficient is similar to that of YAG. Nd^{3+} ion [1,2,5,6] is the most popular ion for laser application. Nd^{3+}:Y_2O_3 ceramic with laser output was obtained by Lu et al. [7] in 2001.

Obtaining transparent ceramics requires a final density of near 100% [8] and thus a strict control of the characteristics of initial powders is required [9–11]. Actually, the sinterability of ceramic powder is highly dependent on their specificities [12,13] such as grain size, size distribution, grain morphology and grain agglomeration state. Messing and Stevenson [14] thought the most effective approach to get pore free ceramics is to ensure that all pores are smaller than the average particle size after the starting powder is consolidated into the desired shape. Well dispersed nano-powder is always preferred for the sintering of transparent ceramics [15]. Mono-dispersed spheres particles are also required in consideration of particle packing and uniform microstructure afforded by a narrow particle size distribution. So it is always a challenge to find a synthesis route to get mono-dispersed powders for transparent ceramic. Mono-dispersed alumina hydroxide has been prepared by Sacks et al. [16]. But the particle size distribution was broad. Mono-sized alumina hydroxide powder was originally obtained by urea homogeneous co-precipitation method [17]. Mono-dispersed Y/Ce powder was obtained by Aiken et al. [18]. To obtain mono-sized particles, a careful control of the precipitation process is needed, including the temperature, hold time and concentration.

The first transparent yttria ceramic was prepared by Lefever and Matsho in 1967 [19]. The sample was densifiy by hot pressing at 950 °C with 70 MPa using LiF as sintering additive. The addition of LiF was responsible for the formation of liquid phase during sintering.

In 2002 Ikegami et al. [10] reported the fabrication of transparent yttria ceramics from the low temperature synthesized yttrium hydroxide coral powder with a diameter under 100 nm. They made transparent yttria ceramic by adding sulfate ammonium as the sintering additive. After sintering at 1700 °C

* Corresponding author. Tel.: +86 21 5241 2165; fax: +86 21 5241 3122.
E-mail address: wyu@mail.sic.ac.cn (Y. Huang).

0272-8842/$36.00
doi:10.1016/j.ceramint.2011.06.008

under vacuum, the transmittance was higher than 35% at 800 nm. The average grain size after sintering was about 20 μm.

In this paper, mono-dispersed Nd:Y_2O_3 powder was prepared by homogeneous co-precipitation method using urea to adjust the solution pH. The effect includes temperature, aging time, and the concentration of urea etc. The properties of yttria powder were investigated.

2. Experimental procedure

2.1. Powder preparation and compaction

Yttria powder and appropriate amount of neodymium oxide powder (99.99%, Shanghai YueKai New Materials Co. Ltd., Shanghai) were dissolved in nitric acid, and then diluted with suitable deionized water to prepare the nitrate solution (3.2 L in beaker), which was used as the mother solution. Precursors were prepared by adding urea and 0.05 wt% ammonium sulfate, and put into the oven at 90 °C for several hours, or into a microwave oven (700 W) operating for several minutes. Then the gel was washed with water for four times to remove the byproducts. After washing, the gel was frozen and dried by freeze-drying machine (Beijing Boyikang Experiment Instrument Co. Ltd., FD-1A-50, Beijing). The precursors were calcined at different temperature. The obtain neodymium doped yttria powder was then uniaxially compacted in ¢ 20 mm steel die at 40 MPa followed by isostatically pressing at a pressure of 200 MPa.

2.2. Characterization

Particle size of initial lanthanum doped yttria was determined by X-ray diffraction (Model D/MAX-2550V, Rigaku, Japan), and field emission scanning electron microscopy (FESEM, JSM-6700F, JEOL, Tokyo, Japan). FTIR (7199-CFT-IR, Nicolet, American) was used to characterize the precursor calcined at different temperature. The content of neodymium doping was calculated by chemical analysis method. BET was used to obtain the specific surface area of the calcined yttria. Optical microscope was used to determine the grain size after sintering, at least 300 grains was measured to get the mean size. The grain sizes were calculated using the linear-intercept method and calculated from $G = 1.5L$, where G is the average grain size and L is the average intercept length. Mirror-polished samples were etched by 20% boiling HCl for 1 min. Mirror-polished samples on both surfaces were used to measure optical transmittance (Model U-2800 Spectrophotometer, Hitachi, Japan). Archimedes method was utilized for measuring the densities of samples.

3. Results and discussion

3.1. Synthesis of mono-dispersed spherical powder

Mono-dispersed spherical Nd:Y_2O_3 powder were obtained at different conditions. Fig. 1 shows micrographs of the particles at different conditions.

Fig. 2 shows the relationship between aging time and the particle diameter. With the increase in aging time, the particles grow up from 250 nm to 1350 nm progressively. All the particles were spherical and mono-dispersion (such as Fig. 1(a)) except for samples aged for 2 h, which was coagulated sphere (Fig. 1(b)). The sphere diameter was 250 ± 35 nm.

Fig. 3 shows the relationship between the ratio of [urea]/[Y^{3+}] and the particle diameter. The particle diameter decreased quickly from 700 nm (Fig. 1(a)) to 180 nm when the [urea]/

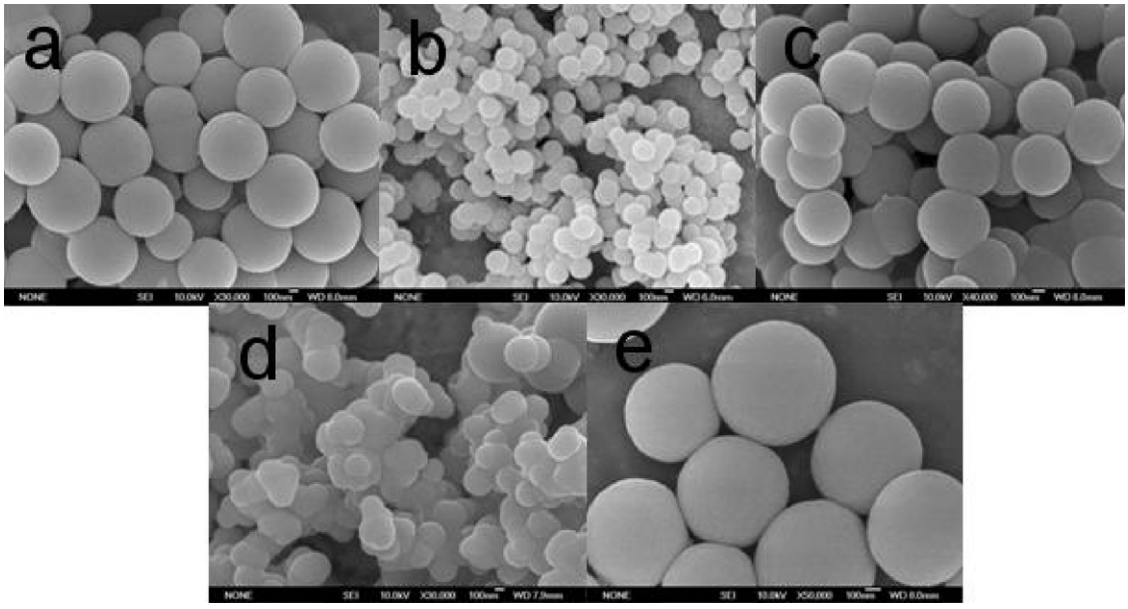

Fig. 1. SEM micrographs of particles obtained (a) aging 7 h at 90 °C, a solution 2.5×10^{-2} mol/L $Y(NO_3)_3$, 1.25×10^{-3} mol/L $Nd(NO_3)_3$, and 0.16 mol/L urea. (b) Aging 2 h at 90 °C, a solution 2.5×10^{-2} mol/L $Y(NO_3)_3$, 1.25×10^{-3} mol/L $Nd(NO_3)_3$, and 0.16 mol/L urea. (c) Aging 7 h at 90 °C, a solution 2.5×10^{-2} mol/L $Y(NO_3)_3$, 1.25×10^{-3} mol/L $Nd(NO_3)_3$, and 1.2 mol/L urea. (d) Aging 7 h at 90 °C, a solution 8×10^{-2} mol/L $Y(NO_3)_3$, 4×10^{-3} mol/L $Nd(NO_3)_3$, and 0.16 mol/L urea. (e) Aging 4 h at 90 °C, a solution 2.5×10^{-2} mol/L $Y(NO_3)_3$, 3.75×10^{-3} mol/L $Nd(NO_3)_3$, and 0.16 mol/L urea.

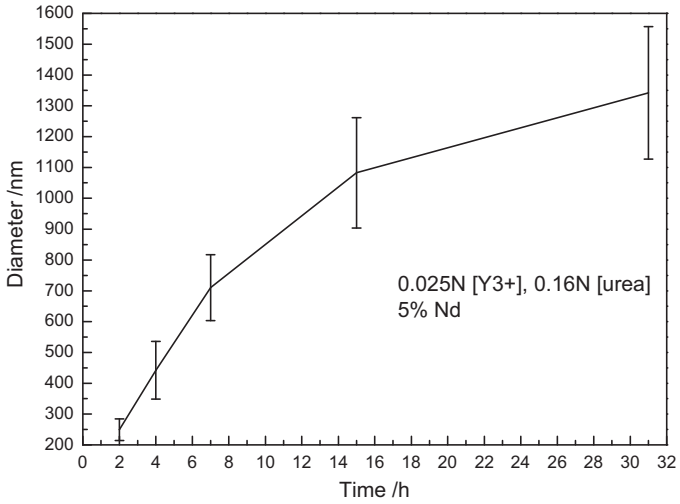

Fig. 2. The relationship between aging time and the particle diameter (constant concentration of 0.16 mol/L urea, 2.5×10^{-2} mol/L $Y(NO_3)_3$ and 1.25×10^{-3} mol/L $Nd(NO_3)_3$).

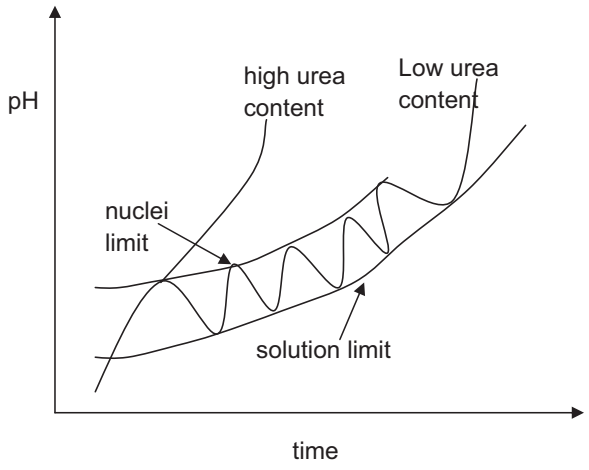

Fig. 4. The nuclei formation progress of urea homogeneous co-precipitation.

$[Y^{3+}]$ ratio increased from 7 to 120. When the ratio was 48, the particle microphotograph was shown in Fig. 1(c), the diameter was 509 ± 31 nm. The higher $[urea]/[Y^{3+}]$ ratio was, the smaller the particle diameter was. More urea might lead to the quick increase in solution pH, and probably more nucleus will be developed. As the concentration of $[Y^{3+}]$ was fixed, more nucleuses might lead to the decrease in particle size. The particles obtained at higher $[urea]/[Y^{3+}]$ ratio such as 120 were spherical but not mono-dispersed.

It was found that with the increase in $[urea]/[Y^{3+}]$ ratio, the particle distribution becomes narrow. Fig. 4 shows the nuclei formation progress of urea homogeneous co-precipitation. When the $[urea]/[Y^{3+}]$ ratio was low, less carbonate were released with time. With the forming and growing of nucleus, the pH value was low again not enough to form nuclei continually. Then the nuclei formation was stopped. And it restarted when the released carbonate radical was enough again. The nuclei formation happened many times when the $[urea]/[Y^{3+}]$ ratio was low, which led to the broad distribution of particle size. If the $[urea]/[Y^{3+}]$ ratio is high enough, the nuclei forms at one time, mono-sized particle would be produced [20].

Fig. 5 shows the relationship between $[Y^{3+}]$ concentration and the particle diameter. When the $[Y^{3+}]$ concentration increased from 0.01 mol/L to 0.025 mol/L, the particle diameter decreased from about 966 ± 132 nm to 766 ± 143 nm (Fig. 1(a)). This trend continued up to $[Y^{3+}]$ concentration of 0.04 mol/L $[Y^{3+}]$ when the particles tend to form coagulated spheres or plate-like configurations (Fig. 1(d)). So the $[Y^{3+}]$ concentration should not exceed 0.04 mol/L in order to obtain mono-dispersed spherical particles.

Fig. 6 shows the relationship between $[Nd^{3+}]/Y_2O_3$ ratio and the particle diameter. The more Nd was added, the larger the particle diameter was. Fig. 1(a) was the microphotograph of 5% Nd, while Fig. 1(e) was the microphotograph of 15% Nd. The

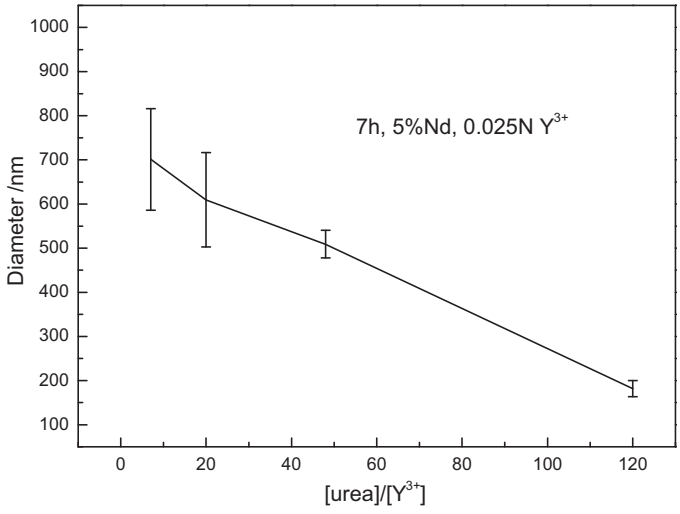

Fig. 3. The relationship between $[urea]/[Y^{3+}]$ and the particle diameter (constant concentration of 2.5×10^{-2} mol/L $Y(NO_3)_3$ and 1.25×10^{-3} mol/L $Nd(NO_3)_3$ and 4 h at 90 °C).

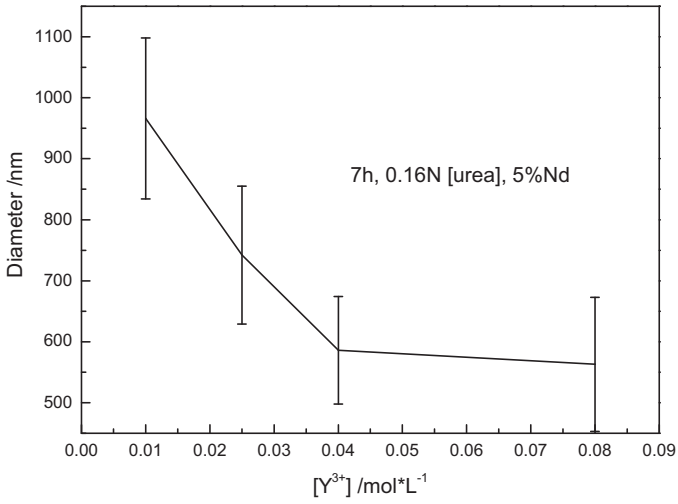

Fig. 5. The relationship between $[Y^{3+}]$ concentration and the particle diameter (constant concentration of 0.16 mol/L urea and 5% $Nd(NO_3)_3$ and 7 h at 90 °C).

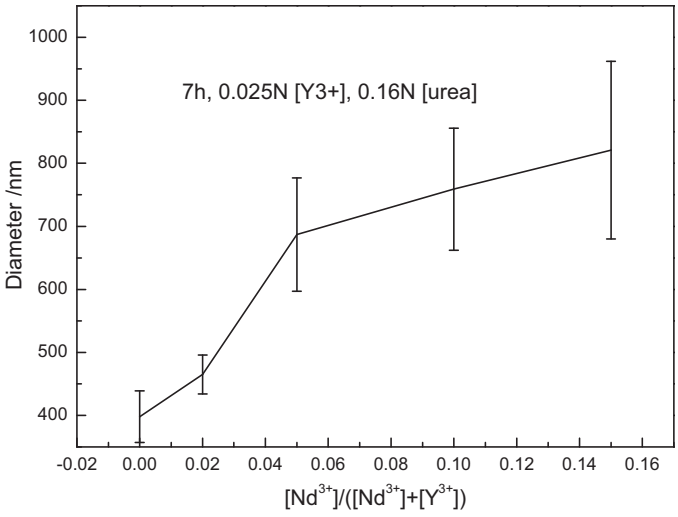

Fig. 6. The relationship between $[Nd^{3+}]$ ratio and the particle diameter (constant concentration of 0.16 mol/L urea, 2.5×10^{-2} mol/L $Y(NO_3)_3$ and 7 h at 90 °C).

particle size distribution dispersion becomes wide with the increase of Nd/Y_2O_3 ratio.

Considering all the parameters that influence the particle size and morphology, mono-sized 2% $Nd:Y_2O_3$ powder was prepared at certain conditions(a solution of 2.5×10^{-2} mol/L $Y(NO_3)_3$, 5×10^{-4} mol/L $Nd(NO_3)_3$, and 1.2 mol/L urea, aging at 90 °C for7 h). Fig. 7 shows the microphotographs of the $Nd:Y_2O_3$ powders. Fig. 7(a) was the microstructure of the precursors before calcinations. Particle size of the amorphous sphere was 465 ± 35 nm. The size distribution was narrow enough to call it mono-sized particle. After calcinations, the particle size decreased to 374 ± 25 nm (Fig. 7(b)). There is about 19.6% shrinkage in diameter, which means 46% shrinkage in volume. Using this favorite conditions (a solution of 2.5×10^{-2} mol/L $Y(NO_3)_3$, 5×10^{-4} mol/L $Nd(NO_3)_3$, and 1.2 mol/L urea), the experiment was operated in a microwave oven boiling for 2 min. Fig. 7(c) shows the microstructure of microwave oven precursors, its size was about 95 nm and it was also near-mono-sized sphere particle. Fig. 7(d) shows the microstructure of $Nd:Y_2O_3$ after calcinations from Fig. 7(c). Its size was 72 nm, still it remained mono-size spherical shape, and less aggregation was observed. The white color on the sphere was due to the crystalline of $Nd:Y_2O_3$. Microwave oven method can make the particle finer, and it is more effective. Fig. 8 shows the microphotograph and its electronic diffraction of one $Nd:Y_2O_3$ particle. It can be seen that the spherical particle was composed of many small crystals. The crystal size was about 25 nm.

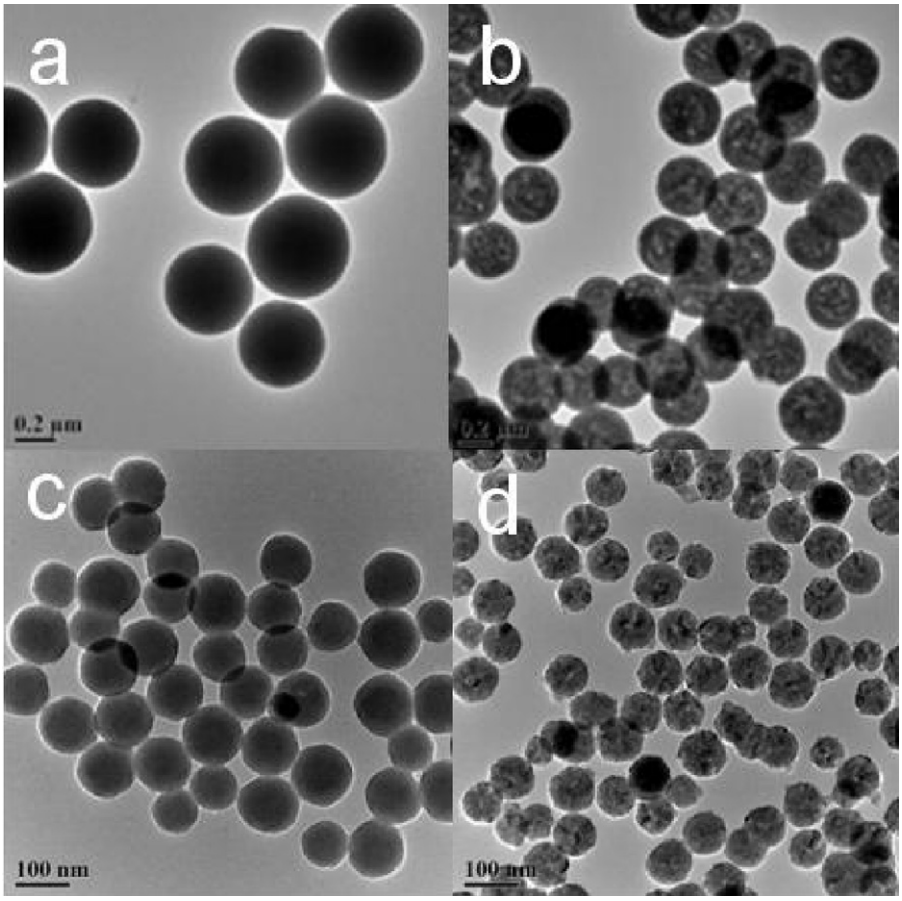

Fig. 7. TEM microphotographs of mono-sized particles from a solution 2.5×10^{-2} mol/L $Y(NO_3)_3$, 5×10^{-4} mol/L $Nd(NO_3)_3$, and 1.2 mol/L urea, obtained by aging 7 h at 90 °C, before (a) and after (d) calcination at 850 °C for 3 h, and by reacting in a microwave oven (700 W) boiling for 2 min, before (c) and after (d) calcination at 850 °C.

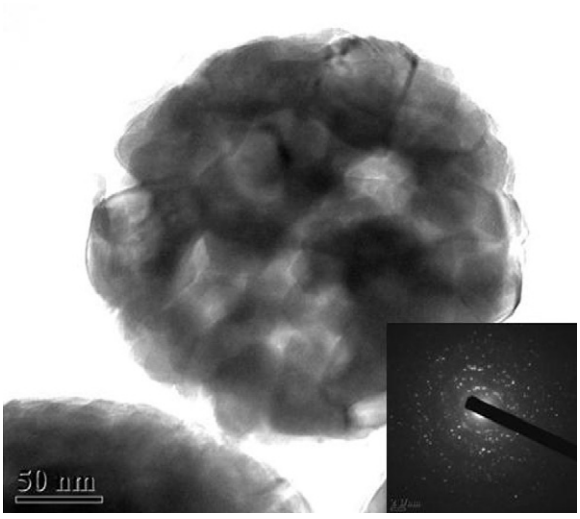

Fig. 8. TEM microphotograph of one spherical Nd:Y_2O_3 powder and its electronic diffraction.

Fig. 9 shows the TG–DTA curves of the dried precipitate precursor obtained from urea co-precipitation method. It was observed at the TG curve that there are three stages of weight loss in the temperature ranges from 100 to 200 °C, 220 to 580 °C and 580 to 700 °C, respectively. These three stages can be corresponded to one endothermic peak at 173 °C, a shallow peak at about 300 °C, and an endothermic doublet at 625 and 663 °C in DTA curve. The mass loss in total 3 steps was about 42%. Considering its 48% shrinkage in volume (Fig. 6), the powder density of one particle increased after calcinations. It can be seen that most of the weight loss occurred before 700 °C. The first endothermic peak at 173 °C is the result of the release of water. The shallow peak may be due to the decomposition of carbonates. And the doublet endothermic peak for the spherical particles could be due to simultaneous processed of crystallization and chemical decomposition.

Additional useful information could be deduced from TG–DTA curve is the formula of the precursor. The weight losses from 100 to 200 °C, 220 to 580 °C and 580 to 700 °C are 10.9, 8.4 and 22.6%, respectively. So the chemical formula of the precursor can be deduced as $R_2(OH)CO_3 \cdot H_2O$ (R = Y and Nd).

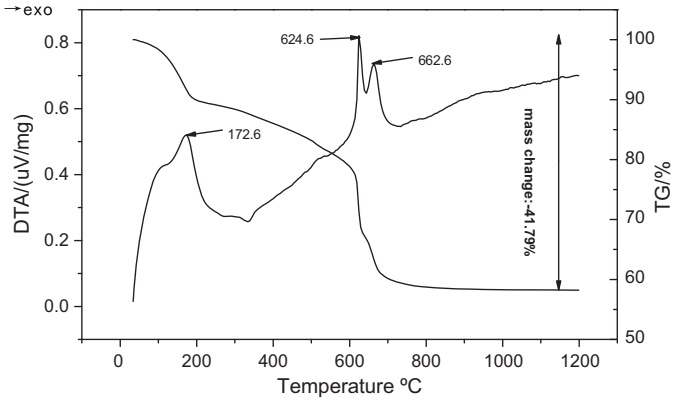

Fig. 9. TG–DTA curves of the precursors (10 °C/min).

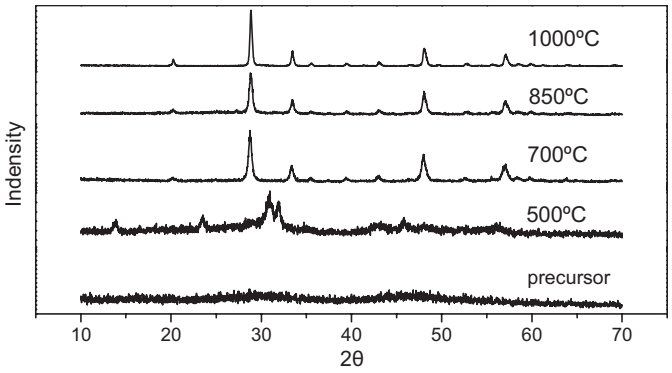

Fig. 10. XRD profiles of the precursors before and after calcinations at different temperatures.

Fig. 10 shows the XRD pattern of the original precursor and precursors calcined at different temperature (500, 700, 850, and 1000 °C) for 4 h. The spherical particles show amorphous in the XRD pattern. When it was calcined at 500 °C for 4 h, the particles showed an intermediate state, which could not be identified. The yttria phase appeared after calcining at 700 °C for 4 h. The peaks can be indexed as cubic yttria phase JCPDS No. 65-3178, no peaks for Nd are detected. With the increase in the calcinations temperature, the peaks became sharper. That is because the crystal grew bigger at high temperature. The crystalline sizes of those spherical particles were 18, 20, and 43 nm responded to 700, 850, and 1000 °C calcinations.

Fig. 11 shows the IR spectra of Nd:Y_2O_3 precursors calcined at different temperature (850 °C, 700 °C, 500 °C and original precursors). Fig. 11(a) is the curve of original powder, it has a distinct carbonate bands (1350–1600 and 860–880 cm^{-1}), and OH stretching vibrations (3000–3500 cm^{-1}), a water hydration band (1650 cm^{-1}). After calcinations at 500 °C in Fig. 11(b), OH stretching vibrations was weak. In Fig. 11(c), after calcinations at 700 °C no carbonate bands were detected. And the Y–O absorption bands (562 and 445 cm^{-1}) were observed.

3.2. Compaction

Fig. 12 shows the fracture surface of the mono-sized Nd:Y_2O_3 and the well-known ammonia precipitation [10] Nd:Y_2O_3 green bodies. All the powders were cold isostatic pressing at 250 MPa. In Fig. 12(a), it can be seen that all the mono-sized particles

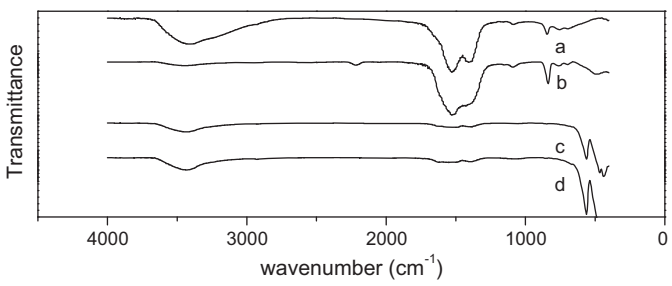

Fig. 11. IR spectra of Nd doped yttria spherical sample: (a) original precursor and the powder calcined at (b) 500 °C, (c) 700 °C, and (d) 850 °C.

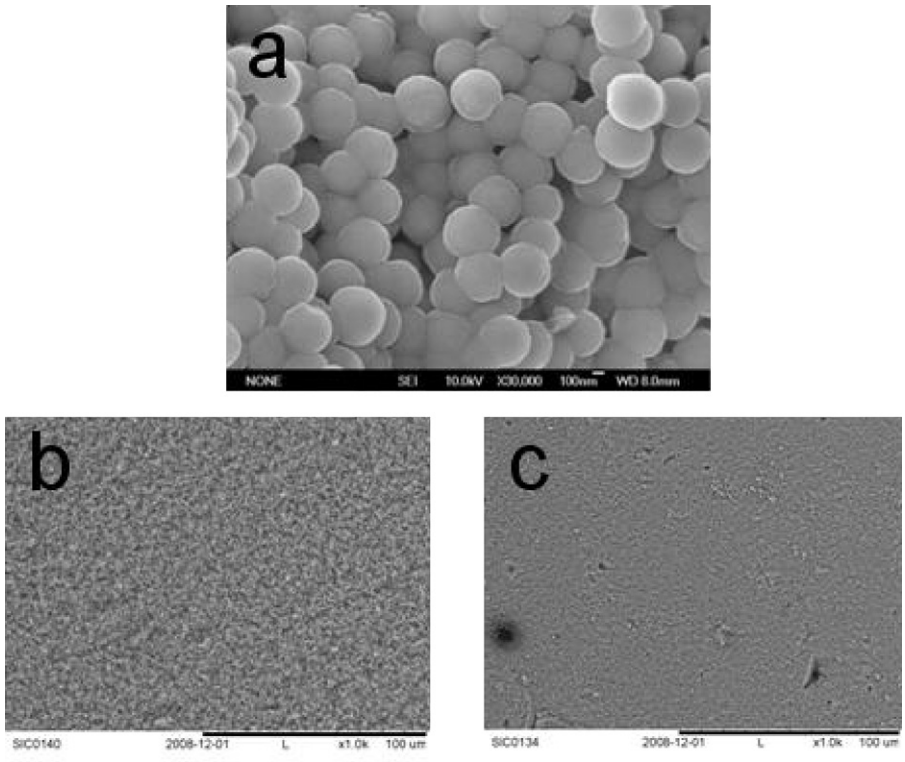

Fig. 12. EPMA micrograph of the fracture of the mono-size Nd:Y_2O_3 green-body (a) 30,000×, (b) 1000× and ammonia precipitation Nd:Y_2O_3 green-body 1000×.

accumulated closely. The sphere particles transformed a little in order to full the residual space after CIP. In Fig. 12(b), there was no obviously defect in the uniform mono-sized particle green body, while in Fig. 12(c) there were many huge defects in the ammonia precipitation powder green body, whose particle size was about 50 nm. Those defects [14] will evolve into large pores (larger than the average particle size), that compromises the sintering to full density. The relative green densities of the two different green bodies were 51% and 55% for mono-sized powder and ammonia precipitation powder, respectively.

4. Concluding remarks

Mono-sized Nd:Y_2O_3 powder was prepared by homogeneous precipitation method in aqueous solution using urea to adjust the solution pH. The particle diameter could be tailored through the control of the preparation parameters.

The uniform green bodies can be obtained which is suitable for the subsequent sintering.

Acknowledgement

This work was supported by the National Natural Science Foundation of China (No. 50990301), and the State Key Laboratory of High Performance Ceramics and Superfine Microstructures.

References

[1] V. Lupei, A. Lupei, A. Ikesue, Transparent polycrystalline ceramic laser materials, Opt. Mater. 30 (11) (2008) 1781–1786.
[2] C. Greskovich, J.P. Chernoch, Improved polycrystalline ceramic lasers, J. Appl. Phys. 45 (10) (1974) 4495–4502.
[3] K. Takaichi, H. Yagi, J.R. Lu, J.F. Bisson, A. Shirakawa, K. Ueda, T. Yanagitani, A.A. Kaminskii, Highly efficient continuous-wave operation at 1030 and 1075 nm wavelengths of LD-pumped Yb^{3+}:Y_2O_3 ceramic lasers, Appl. Phys. Lett. 84 (3) (2004) 317–319.
[4] A. Lupei, V. Lupei, T. Taira, Y. Sato, A. Ikesue, C. Gheorghe, Energy transfer processes of Nd^{3+} in Y_2O_3 ceramic, in: International Conference on Luminescence and Optical Spectroscopy of Condensed Matter, Budapest, Hungary, (2002), pp. 72–76.
[5] J. Li, Y.S. Wu, Y.B. Pan, L.Q. An, J. Zhang, S.W. Wang, J.K. Guo, Fabrication and laser performance of 1.3 at% Nd:YAG transparent ceramics, J. Inorg. Mater. 22 (2007) 798–802.
[6] A. Ikesue, T. Kinoshita, K. Kamata, K. Yoshida, Fabrication and optical properties of high-performance polycrystalline Nd:YAG ceramics for solid-state lasers, J. Am. Ceram. Soc. 78 (4) (1995) 1033–1040.
[7] J.R. Lu, J.H. Lu, T. Murai, K. Takaichi, T. Uematsu, K. Ueda, H. Yagi, T. Yanagitani, A.A. Kaminskii, Nd^{3+}:Y_2O_3 ceramic laser, Japanese, J. Appl. Phys. Part 2 – Lett. 40 (12A) (2001) L1277–L1279.
[8] G. Bernard-Granger, C. Guizard, L. San-Miguel, Sintering behavior and optical properties of yttria, J. Am. Ceram. Soc. 90 (9) (2007) 2698–2702.
[9] N. Saito, S. Matsuda, T. Ikegami, Fabrication of transparent yttria ceramics at low temperature using carbonate-derived powder, J. Am. Ceram. Soc. 81 (8) (1998) 2023–2028.
[10] T. Ikegami, J.G. Li, T. Mori, Y. Moriyoshi, Fabrication of transparent yttria ceramics by the low-temperature synthesis of yttrium hydroxide, J. Am. Ceram. Soc. 85 (7) (2002) 1725–1729.
[11] Y. Rabinovitch, C. Bogicevic, F. Karolak, D. Tetard, H. Dammak, Freeze-dried nanometric neodymium-doped YAG powders for transparent ceramics, J. Mater. Process. Technol. 199 (1–3) (2008) 314–320.
[12] P.L. Chen, I.W. Chen, Sintering of fine oxide powders. 1. Microstructural evolution, J. Am. Ceram. Soc. 79 (12) (1996) 3129–3141.
[13] P.L. Chen, I.W. Chen, Sintering of fine oxide powders. 2. Sintering mechanisms, J. Am. Ceram. Soc. 80 (3) (1997) 637–645.
[14] G.L. Messing, A.J. Stevenson, Toward pore-free ceramics, Science 322 (5900) (2008) 383–384.

[15] Y.L. Kopylov, V.B. Kravchenko, A.A. Komarov, Z.M. Lebedeva, V.V. Shemet, Nd:Y_2O_3 nanopowders for laser ceramics, Opt. Mater. 29 (10) (2007) 1236–1239.

'[16] M.D. Sacks, T.-Y. Tseng, S.Y. Lee, Thermal decomposition of spherical hydrated basic aluminum sulfate, Am. Ceram. Soc. Bull. 63 (2) (1984) 301–310.

[17] J.L. Shi, J.H. Gao, Z.X. Lin, Formation of monosized spherical aluminum hydroxide particles by urea method, Solid State Ionics 32–33 (pt 1) (1989) 537–543.

[18] B. Aiken, W.P. Hsu, E. Matijev, Preparation and properties of monodispersed colloidal particles of lanthanide compounds: III, yttrium(III) and mixed yttrium(III)/cerium(III) systems, J. Am. Ceram. Soc. 71 (10) (1988) 845–853.

[19] R.A. Lefever, J. Matsko, Transparent yttrium oxide ceramics, Mater. Res. Bull. 2 (9) (1967) 865–869.

[20] E. Matijevic, Production of monodispersed colloidal particles, Mater. Sci. 15 (1) (1985) 483.